Scientia Iranica B (2014) 21(4), 1451–1460

SCIENTIA IRANICA

Sharif University of Technology
Scientia Iranica
Transactions B: Mechanical Engineering
www.scientiairanica.com

Research Note

Spacecraft attitude and system identification via marginal modified unscented Kalman filter utilizing the sun and calibrated three-axis-magnetometer sensors

M. Kiani and S.H. Pourtakdoust*

Center for Research and Development in Space Science and Technology, Sharif University of Technology, Tehran, P.O. Box 11155-9567, Iran

Received 9 May 2012; received in revised form 31 October 2013; accepted 30 December 2013

KEYWORDS
Attitude determination; Inertia matrix identification; Sensor calibration; Reduced sigma point Kalman filter; Marginal filter; Unscented Kalman filter.

Abstract. This paper deals with the problems of attitude determination, parameter identification and reference sensor calibration simultaneously. An LEO satellite's attitude, inertia tensor as well as calibration parameters of Three-Axis-Magnetometer (TAM) including scale factors, misalignments and biases along three body axes are estimated during a maneuver designed to satisfy the condition of persistency of excitation. The advanced nonlinear estimation algorithm of Unscented Kalman Filter (UKF) is a good choice for nonlinear estimation problem of attitude determination, but its computational cost is considerably larger than the widespread low accurate Extended Kalman Filter. Reduced Sigma Point Filters provide good solutions and also decrease the run time of the UKF. However, in contrast to the nonlinear problem of attitude determination, parameter identification and sensor calibration have linear dynamics. Therefore, a new marginal UKF is proposed that combines utility of Kalman Filter with Modified UKF (MUKF) which is based on Schmidt orthogonal algorithm. The proposed Marginal MUKF (MMUKF) utilizes only 14 sigma points to achieve the complete 25-dimensional state vector estimation. Additionally, a Monte Carlo simulation has demonstrated a good accuracy and lower computational burden for concurrent estimation of attitude, inertia tensor as well as TAM calibration parameters utilizing MMUKF with respect to the sole utilization of the UKF.

1. Introduction

Acceptable performance of a variety of tasks of a spacecraft such as photography, pointing, data transmission, etc. are strongly dependent on the accurate knowledge of spacecraft attitude, attitude time rate, and system parameters. Moments Of Inertia tensor (MOI) is an important system parameter that significantly affects satellite rotational dynamics. In this sense, identification of MOI is considered a vital task for many spacecrafts. Since more accurate measurements provide higher pointing performance, the identification of the parameters of measurement system has significant importance. As operational conditions of satellites vary in orbit, from those presumed in simulations, on-line estimation of dynamic and measurement systems' parameters is more important than off-line determination. Estimation of spacecraft attitude and its rate is regarded a task of Attitude Determination (AD) subsystem, while estimation of moments of inertia is the task of system Parameter Identification Module (PIM), and the sensor alignment parameters is estimated by Measurement Sensor Calibration (MSC)

*. *Corresponding author. Tell.: +98 21 66164601; Fax: +98 21 66022731*
E-mail addresses: m_kiani@ae.sharif.ir (M. Kiani); pourtak@sharif.edu (S.H. Pourtakdoust)

module. A lot of studies have been devoted to each of these topics in the past decades. Identification of MOI is the only concentration of Refs. [1-4]. While Wertz and Lee [1] have utilized least square method to identify MOI of a satellite, Zarringhalam et al. [2] have compared recursive least square, recursive Kalman filter, gradient, and Extended Kalman Eilter (EKF) for estimation of mass, MOI, and location of center of gravity. They have concluded that EKF is the most reliable method for online identification of vehicle inertial parameters. Mohammed et al. [5] have described various steps of design and implementation of an attitude determination system based on Kalman filter for Alsat-1. Gyro calibration as well as AD based on a vector sensor like star tracker using EKF or Unscented Kalman Filter (UKF) is considered in [6-9]. [10-12] have focused just on MSC of Gyro, star tracker, and Three-Axis-Magnetometer (TAM) using recursive estimation algorithms like EKF. Soken et al. [13] have proposed a reconfigurable UKF to calibrate TAM parameters and then estimate attitude of a pico-satellite based on rate gyro and TAM measurements. In contrast with above references which have mainly focused on one of the mentioned tasks or at most two of them, Kutlu et al. [14] has utilized gyro measurements, as well as TAM and sun sensor data for estimation of attitude, and bias vector of gyro via EKF. Subsequently, the center of mass position vector and the inertia tensor were determined using least square method, but Myung et al. [15] used a single algorithm to calibrate gyro measurements, determine attitude of the satellite and identify MOI simultaneously using EKF based on gyro measurements and star tracker. These references are common in utilizing expensive and heavy star tracker sensor in order to calibrate the gyro. Since cost and weight are serious constraints for a large number of the present and future space projects, utilizing light and inexpensive sensors is becoming an attraction. Lowering weight and cost must not degrade the performance of navigation and control subsystems, so sensors data fusion and precise calibration of sensor packages utilizing reliable advanced estimation algorithms are effective ideas to achieve acceptable performance.

The presented paper focuses on AD, MSC and PIM, simultaneously. Measurement data is provided by a centralized fusion of TAM and sun sensor. TAM measurements are contaminated by various sources of error such as scale factor, misalignment, bias, as well as random white noise. As the governing equations of kinematics and dynamics of satellite are nonlinear and the state space equations of parameters are linear, a marginal filter, that is a combination of KF and Modified UKF called MMUKF, is developed for accurate and fast estimation process.

The structure of this paper is organized as follows. Attitude kinematics and dynamics are described in Section 2. Measurement model is introduced in Section 3. Section 4 is devoted to development of marginal modified UKF. Section 5 provides the numerical simulation results. Section 6 summarizes the results and draws recommendations for further research.

2. Attitude kinematics and dynamics

2.1. Attitude dynamics

The nonlinear attitude dynamics of a rigid satellite can be described by the well known Euler law. Expressing this law in the satellite body coordinate system results in [16]:

$$\dot{\vec{\omega}}_{\mathrm{BI}} = I_B^{B^{-1}}(\vec{\tau} - \vec{\omega}_{\mathrm{BI}} \times I_B^B \vec{\omega}_{\mathrm{BI}}) + \vec{w}_\omega,$$

$$\vec{\tau} = \vec{\tau}_c + \vec{\tau}_d, \tag{1}$$

where:

$$I_B^B = \begin{bmatrix} I_{xx} & I_{xy} & I_{xz} \\ I_{xy} & I_{yy} & I_{yz} \\ I_{xz} & I_{yz} & I_{zz} \end{bmatrix},$$

$\vec{w}_\omega$ is the process noise taken as a zero mean Gaussian white with covariance $Q_{\vec{\omega}}$. It is assumed that aerodynamic drag and gravity gradient forces are the most effective forces producing torques for a LEO satellite.

2.2. Attitude kinematics

Attitude kinematics describes how the attitude of a satellite changes under the influence of its angular velocity. There are various methods to represent attitude of a body [17]. Quaternion parameters are the most desired and widely used method to this aim. This is due to linear propagation behavior of the quaternion as well as its non-singular characteristics. The constraint of unit norm is the only disadvantage that must be observed. Quaternion parameters are propagated in time as [18]:

$$\{\dot{q}\} = \frac{1}{2}\Omega(\vec{\omega}_{\mathrm{BI}})\{q\}, \tag{2}$$

where:

$$\Omega(\vec{\omega}_{\mathrm{BI}}) = \begin{bmatrix} K\varepsilon & \omega_z & -\omega_y & \omega_x \\ -\omega_z & K\varepsilon & \omega_x & \omega_y \\ \omega_y & -\omega_x & K\varepsilon & \omega_z \\ -\omega_x & -\omega_y & -\omega_z & K\varepsilon \end{bmatrix},$$

$$\{q\} = [q_1\ q_2\ q_3\ q_4], \quad K = cte, \quad \varepsilon = 1 - \{q\}^T\{q\},$$

q_4 is the scalar part of the quaternion vector. Diagonal elements of $\Omega(\vec{\omega}_{\mathrm{BI}})$ guarantee maintenance of unit norm of the quaternion even in the presence of rounding errors. K is a constant selected such that $K\Delta t \leq 1$ (Δt is integration time step).

2.3. Disturbing moments

The aerodynamic drag induced disturbing torque in the satellite body coordinate system is modeled as:

$$\vec{\tau}_a = D\left([\vec{u}_v]^B \times [\vec{s}_{cp}]^B\right), \tag{3}$$

where $[\vec{u}_v]^B$ is the unit vector of satellite velocity in the body coordinate system, $[\vec{s}_{cp}]^B$ is the position vector of the satellite pressure center with respect to satellite center of mass, and $D = 0.5\rho v^2 SC_D$. It is assumed that required data regarding the satellite position and velocity is provided via the orbit determination subsystem.

Also, the gravity gradient torque is modeled as:

$$\tau_{gg} = \frac{3\mu}{r^3}(c_3 \times I_B^B c_3), \tag{4}$$

where c_3 is the third column of the inertial to body transformation matrix.

3. Measurement model

Measurement system consists of a centralized fusion of TAM and sun sensor. TAM measures the Earth magnetic field modeled as:

$$[\vec{B}_{\text{meas}}]^B = (E+M)T^{BI}[\vec{B}_{\text{Model}}]^l + \vec{b} + \vec{v}_B, \tag{5}$$

where:

$$M = \begin{bmatrix} \lambda_1 & \delta_{12} & \delta_{13} \\ \delta_{21} & \lambda_2 & \delta_{23} \\ \delta_{31} & \delta_{32} & \lambda_3 \end{bmatrix}, \tag{6}$$

E is a 3×3 identity matrix and T^{BI} is the inertial (I) to body (B) transformation matrix, defined in terms of its corresponding quaternion parameters:

$$T^{\text{BI}} = \begin{bmatrix} q_1^2-q_2^2-q_3^2+q_4^2 & 2(q_1q_2+q_3q_4) & 2(q_1q_3-q_2q_4) \\ 2(q_1q_2-q_3q_4) & -q_1^2+q_2^2-q_3^2+q_4^2 & 2(q_2q_3+q_1q_4) \\ 2(q_1q_3+q_2q_4) & 2(q_2q_3-q_1q_4) & -q_1^2-q_2^2+q_3^2+q_4^2 \end{bmatrix}, \tag{7}$$

$\vec{B}_{\text{Model}}$ is a function of the satellite orbital position, derived from the International Geomagnetic Reference Field (IGRF) model. $\vec{v}_B$ is the measurement noise of TAM, assumed to be zero mean white Gaussian with variance σ_B^2 along each axis.

Sun sensor is the other reference sensor used in our measurement package. It is assumed that calibration parameters of sun sensor are negligible in comparison with those of TAM. sun sensor measures direction of the sun light with respect to satellite onboard sensor. Its output in body coordinate system is modeled as:

$$[\vec{u}_s]^B = T^{\text{BI}}[\vec{u}_s]^I + \vec{v}_s, \tag{8}$$

$[\vec{u}_s]^I$ is the sun direction vector in inertial coordinate system, and $\vec{v}_s$ is the sun sensor measurement noise modeled as zero mean Gaussian white noise with variance σ_s^2 along each axis. In addition, no correlation is assumed to exist between $\vec{v}_B$ and $\vec{v}_s$.

4. Marginal modified unscented Kalman filter

Nonlinear problem of spacecraft attitude determination is studied extensively in the past decade. Extended Kalman Filter (EKF) is the most desired and widely used algorithm for this application. EKF is based on linearization of nonlinear models of dynamic and measurement systems, so applying EKF to nonlinear problems is usually accompanied with two potential threats of filter divergence and estimation performance degradation. In recent years, more advanced nonlinear filters such as sampling approaches have been developed independent of the need for calculation of Jacobian matrices. Specific disadvantage of these filters is numerical cost requirements, so that only a few certain of them can be applied to actual onboard implementations. Unscented Kalman Filter (UKF) is the most efficient algorithm among them. UKF uses a deterministic set of weighted sigma points to approximate system probabilistic characteristics. Standard UKF uses $2n+1$ sigma points to estimate an n-dimensional state vector. Computational cost of the sample based algorithms like UKF is proportional to the number of required sigma points. Regarding this, and in order to reduce the computational efforts, several strategies known as Reduced Sigma Point Filters (RSPF) have been developed, through lowering number of sigma points, such as the simplex point selection strategies that utilize only $n+2$ points. These strategies contain a zero central point. In contrast to the central point strategies, other schemes have evolved using only $n+1$ equally weighted sigma points, without the need of any central point. It is also proved that [19] equally weighted, negative weighted-free sigma point sets are numerically more stable and accurate while being more efficient. Although RSPFs are efficient algorithms for practical applications, marginalization of partially linear systems, such as that of MSC, can effectively reinforce further reduction in computational complexity. The basic idea behind marginalization is to partition the state vector into two parts of linear $\vec{x}^l$ and $\vec{x}^n$ nonlinear. Using Bayes' rule the linear state variables can then be marginalized out and estimated using the Kalman Filter (KF) that is optimal for linear cases. The nonlinear state variables are estimated using RSPF which is called Modified UKF here. This way, marginal RSPF only needs one set of sigma points that adequately describe the statistic properties of the nonlinear part of the states. This technique is also

referred to as Rao-Blackwellization. While the basic idea of marginal filters and Rao-Blackwellization is seen to have been more utilized for Particle Filters (PF), its application in UKF is new and rare [20].

4.1. Modified Unscented Kalman Filter (MUKF)

It is convenient to introduce Modified UKF (MUKF) before presenting Marginal MUKF (MMUKF) algorithm. As mentioned previously and proved [21], $n+1$ sigma points are sufficient to represent mean and covariance completely. The MUKF is a new simplex Unscented Transform (UT) based on Schmidt orthogonal algorithm. Computational time and effort of this filter is less than UKF, simplex UKF (SUKF), and EKF, but has the same performance as UKF and SUKF. MUKF uses a minimum number of sigma points set with the same weights to provide efficient and unbiased estimates.

The nonlinear discrete time system considered in MUKF can be presented as:

$$\vec{x}_{k+1} = \vec{f}(\vec{x}_k, \vec{u}_k, k) + \vec{w}_k, \tag{9a}$$

$$\vec{z}_k = \vec{h}(\vec{x}_k, k) + \vec{v}_k, \tag{9b}$$

where $\vec{x}_k$ is n-dimensional state vector, $\vec{z}_k$ is m-dimensional observation vector, and $\vec{f}$ and $\vec{h}$ are nonlinear functions. $\vec{w}_k$ and $\vec{v}_k$ are the corresponding process and measurement noise vectors. It is assumed that the noise vectors are zero mean Gaussian white with covariances given by Q_k and R_k, respectively.

At any time index k, the estimation of state vector is represented $\hat{\vec{x}}_k$ and the state covariance is given by P_k. Since P_k is positive definite, its Cholesky decomposition is given by $P_k = S_k S_k^T$, where S_k is a positive lower triangular matrix.

$n+1$ sigma points are selected in three steps as follows [21]:

1. Choose equal weights $\varpi_i = 1/(n+1)$; $i = 1, ..., n+1$.
2. Construct scale vectors as:

$$\Lambda_i = \sqrt{n+1}\Big[\underbrace{[i(i+1)]^{-0.5}, ..., [i(i+1)]^{-0.5}}_{i}, - (\frac{i+1}{i})^{-0.5}, \underbrace{0, ..., 0}_{n-i}\Big].$$

3. Sigma points are arranged in $n \times (n+1)$ matrix, $\chi_k = 1 \otimes \hat{\vec{x}}_k + S_k\Lambda$, where $\otimes$ represents Kronecker product.

Once the sigma points are chosen, they are propagated through the nonlinear dynamic system via:

$$\chi^i_{k+1/k} = f(\chi^i_k, k), \tag{10}$$

where $\chi^i_{k+l/k}$ represents the ith column vector of the matrix $\chi_{k+1/k}$ $(i = 1, 2, ..., n+1)$. Then, the predicted state vector $\hat{\vec{x}}^-_{k+1}$ is computed as the weighted mean of the predicted sigma points:

$$\hat{\vec{x}}^-_{k+1} = \sum_{i=1}^{n+1} \chi^i_{k+1/k}\varpi_i. \tag{11}$$

Predicted S^-_{k+1} (square-root of covariance P^-_{k+1}) will be calculated using QR decomposition and the cholupdate function as below [22]:

$$S^-_{k+1} = \text{qr}\left([\sqrt{\varpi_2}(\chi^{2:n+1}_{k+1/k} - \hat{\vec{x}}^-_{k+1}) \quad \sqrt{Q}]\right), \tag{12}$$

$$S^-_{k+1} = \text{cholupdate}(S^-_{k+1}, \chi^1_{k+1/k} - \hat{\vec{x}}^-_{k+1}, \sqrt{\varpi_1}). \tag{13}$$

Subsequently, the sigma point's matrix is reconstructed:

$$\chi_{k+1} = 1 \otimes \hat{\vec{x}}^-_{k+1} + S^-_{k+1}\Lambda. \tag{14}$$

Each of the predicted sigma points passes through the observation model to produce:

$$\Im_{k+1} = h(\chi^i_{k+1}, k). \tag{15}$$

The predicted measurement and square root of measurement covariance is:

$$\hat{\vec{Z}}^-_{k+1} = \sum_{i=1}^{n+1} \Im^i_{k+1}\varpi_i, \tag{16}$$

$$S_{z,k+1} = \text{qr}\left([\sqrt{\varpi_2}(\Im^{2:n+1}_{k+1} - \hat{\vec{Z}}^-_{k+1}) \quad \sqrt{R}]\right), \tag{17}$$

$$S_{z,k+1} = \text{cholupdate}\left([S_{z,k+1}, \Im^1_{k+1} - \hat{\vec{Z}}^-_{k+1}, \sqrt{\varpi_1}]\right). \tag{18}$$

Cross correlation matrix is determined by:

$$P_{\vec{x}_{k+1}\hat{z}_{k+1}} = \sum_{i=1}^{n+1} \varpi_i[\chi^i_{k+1/k} - \hat{\vec{x}}^-_{k+1}][\Im^i_{k+1} - \hat{\vec{z}}^-_{k+1}]^T. \tag{19}$$

UKF gain is given by:

$$K_{k+1} = \left(P_{\vec{x}_{k+1}\vec{z}_{k+1}}/S^T_{z,k+1}\right)/S_{z,k+1}. \tag{20}$$

The update state mean is given by:

$$\hat{\vec{x}}_{k+1} = \hat{\vec{x}}^-_{k+1} + K_{k+1}(\vec{Z}_{k+1} - \hat{\vec{Z}}_{k+1}). \tag{21}$$

Square root of state covariance update is computed by:

$$U = K_{k+1}S_{z,k+1},$$

$$S_{k+1} = \text{cholup date}(S^-_{k+1}, U, -1). \tag{22}$$

4.2. Marginal Modified UKF (MMUKF)

To introduce MMUKF, the dynamic and measurement systems described in previous sections are rewritten in discrete-time form as:

$$\vec{x}^{n}_{k+1} = f^{n}_{k}(\vec{x}^{n}_{k}) + w^{n}_{k}, \tag{23a}$$

$$\vec{x}^{l}_{k+1} = A^{l}_{k}(\vec{x}^{n}_{k})\vec{x}^{l}_{k} + w^{l}_{k}, \tag{23b}$$

$$\vec{Z}_{k} = h_{k}(\vec{x}^{n}_{k}) + C_{k}(\vec{x}^{n}_{k})\vec{x}^{l}_{k} + v_{k}, \tag{23c}$$

where:

$$\vec{v}_{k} \sim N(0, R_{k}), \qquad w_{k} = \begin{bmatrix} w^{n}_{k} \\ w^{l}_{k} \end{bmatrix} \sim N(0, Q_{k}),$$

$$Q_{k} = \begin{bmatrix} Q^{n}_{k} & 0 \\ 0 & Q^{l}_{k} \end{bmatrix}.$$

$\vec{x}^{n}$ is n_1-dimensional nonlinear part of state vector, $\vec{x}^{l}$ is n_2-dimensional linear part of state vector ($n_1 + n_2 = n$), $\vec{z}_{k}$ is m-dimensional observation vector, and f, h, A^{l} and C are the nonlinear functions. $\vec{w}_{k}$ and $\vec{v}_{k}$ are the corresponding process and measurement noise vectors. Similarly, it is assumed that the noise vectors $\vec{w}_{k}$ and $\vec{v}_{k}$ are zero mean Gaussian (white) with co-variances given by Q_{k} and R_{k}, respectively. The pseudo code of the proposed MMUKF algorithm is presented in Table 1.

5. Simulation studies

This section is devoted to the simulation and estimation of the parameters of dynamic and measurement systems (as part of the augmented state vector), in addition to the pertinent attitude dynamic states. While the nonlinear part of the state vector consists of $\vec{x}^{n} = [\{q\}\ \vec{\omega}^{\mathrm{BI}}\mathrm{MOI}]$, linear part contains $\vec{x}^{l} = [\vec{\lambda}\ \ \vec{\delta}\ \ \vec{b}]$, where $\mathrm{MOI} = [I_{xx}\ I_{yy}\ I_{zz}\ I_{xy}\ I_{xz}\ I_{yz}]$, $\lambda = [\lambda_1\ \lambda_2\ \lambda_3]$, $\vec{\delta} = [\delta_{12}\ \delta_{13}\ \delta_{21}\ \delta_{23}\ \delta_{31}\ \delta_{32}]$, and $\vec{b} = [b_1\ b_2\ b_3]$.

Complete observability of the described system demands satellite maneuver. In other words, in order to estimate MOI and TAM parameters, persistent excitation must be guaranteed. A constant body rate vector or one with constant direction will not satisfy this requirement. As one of the reference maneuver trajectories, satisfying persistent excitation condition, the following rate trajectory is proposed [15] and utilized in this work:

$$\vec{\omega}_{\mathrm{comm}} = \dot{\vartheta}\vec{\Omega} - (1 - \cos(\vartheta))\vec{\Omega} \times \dot{\vec{\Omega}} + \ddot{\vec{\Omega}}\sin(\vartheta),$$

$$\vec{\Omega} = \begin{bmatrix} \sin(\omega_1 t)\sin(\omega_2 t) \\ \cos(\omega_1 t)\sin(\omega_2 t) \\ \cos(\omega_2 t) \end{bmatrix}, \qquad \vartheta = at, \tag{24}$$

where:

$$a = 0.4\pi\ [\mathrm{rad}/s], \quad \omega_1 = 0.01\ [\mathrm{rad}/s],$$

$$\omega_2 = 0.004\ [\mathrm{rad}/s].$$

The reference maneuver trajectory is shown in Figure 1. The overall maneuver time is 15 minutes. Required control torque to implement this command is provided using fuzzy self-tuning PID controller. Figure 2 depicts time history of controller gains and Figure 3 shows the time history of control torque components.

Table 1. The marginalized modified unscented Kalman filter.

1. Initialize for $i = 1, ..., N = n_1 + 1$

$\hat{\vec{x}}^{n}(0) = \hat{\vec{x}}^{n}_{0}, \quad \hat{\vec{x}}^{l}(0) = \hat{\vec{x}}^{l}_{0}, \qquad P(0) = \begin{bmatrix} P^{n}_{0} & 0 \\ 0 & P^{l}_{0} \end{bmatrix} = \begin{bmatrix} S^{n}_{0} S^{n^{T}}_{0} & 0 \\ 0 & P^{l}_{0} \end{bmatrix}; \quad S^{n}_{0} = \mathrm{chol}(P^{n}_{0}, '\mathrm{lower}')$

2. Introducing weight and sigma points matrix

3. Time update

a) Nonlinear part: Eqs. (10)-(13)

b) Linear part:

$\hat{\vec{x}}^{l}_{k+1|k} = A^{l}_{k}\hat{\vec{x}}^{l}_{k|k}$

$P_{k+1|k} = A^{l}_{k}P_{k|k}(A^{l}_{k})^{T} + Q^{l}_{k}$

4.Measurement update

a) nonlinear part: Eqs. (21) and (22)

b) linear part:

$\hat{\vec{x}}^{l}_{k|k} = \hat{\vec{x}}^{l}_{k|k-1} + K_{k}(\vec{Z}_{k} - \vec{h}_{k} - C_{k}\hat{\vec{x}}^{l}_{k|k-1})$

$P_{k|k} = P_{k|k-1} - K_{k}C_{k}P_{k|k-1}$

$K_{k} = P_{k|k-1}C^{T}_{k}(C_{k}P_{k|k-1}C^{T}_{k} + R_{k})^{-1}$

Table 2. Initial simulation conditions.

State	Initial true value	Initial estimated value
Angular velocity (rad/s)	[0 -0.0011 0]	[1e-3 -0.002 1e-3]
Quaternion parameters	[-0.0739 -0.7032 -0.5495 -0.4450]	[0.4063 0.7592 -0.3573 -0.3617]
MOI (kg.m^2)	[200 50 -30 50 240 10 -30 10 100]	[160 20 -20 20 160 -20 -20 -20 160]
Scale factors (ppm)	[5 -1 -2]e+4	[0 0 0]
Misalignments (arcs)	[648 1296 972 648 -648 1296]	[0 0 0 0 0 0]
Bias (nT)	[1500 1000 500]	[0 0 0]

Table 3. Simulated LEO orbit properties.

Element	Value	Element	Value
Semi major axis (km)	7078.145	Eccentricity	0.07
Inclination (deg)	70	Longitude of ascending node (deg)	57
Argument of perigee (deg)	0	Mean anomaly (deg)	0

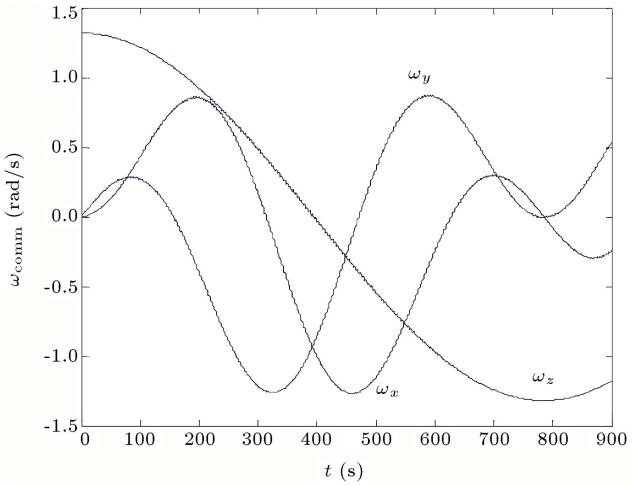

Figure 1. Body angular rate command trajectory.

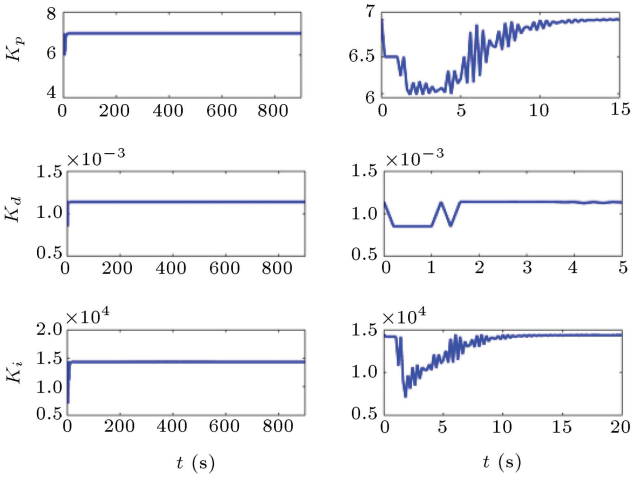

Figure 2. Time history on controller gains (proportional-differential-integral gains).

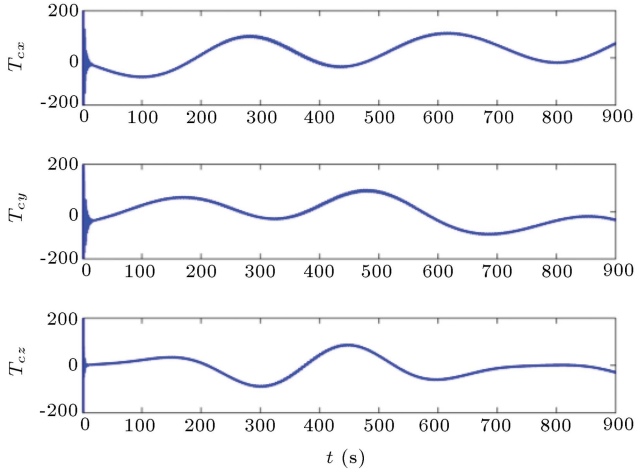

Figure 3. Time history of control torque components.

TAM and sun sensor noises are modeled as zero mean Gaussian white with standard deviations of 50 nT and 1.8°, respectively. The geomagnetic field is modeled using 13th order IGRF 11 [23]. Table 2 shows initial conditions for the simulation. Initial conditions to orbit simulation are also presented in Table 3.

Measurement sampling interval is taken 0.2 sec. Q_k^n is considered as diagonal matrix with diagonal elements equal to $(1e-3)^2$ for body angular velocity and zero for the other nonlinear states. Since parameters are modeled as random constants, Q_k^l is a 12×12 diagonal zero matrix as well.

It is worth mentioning that the standard UKF algorithm was also initially applied to simultaneous PI, MSC and AD, but was subsequently replaced by Modified UKF (MUKF), and then by Marginal Modified UKF (MMUKF) to improve run time effi-

Table 4. Root mean square error of state vector.

State	Root mean square error	State	Root mean square error
Angular velocity (rad/s)	4e-3	Scale factors (ppm)	[250 200 2000]
Rotation angle (deg)	1.4	Misalignments (arcs)	[100 200 800 270 200 200]
MOI (kg.m^2)	[1.6 0.5 0.01 0.5 1.9 0.02 0.01 0.02 0.83]	Bias (nT)	[1 25 4]

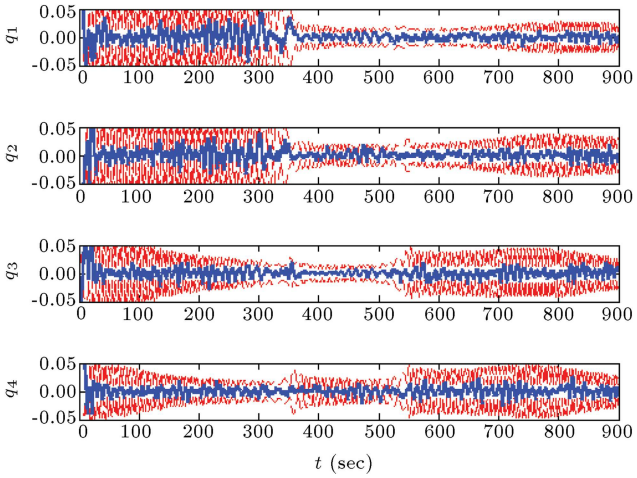

Figure 4. Quaternion parameters estimation errors in MMUKF with $\pm$ 3σ error bounds.

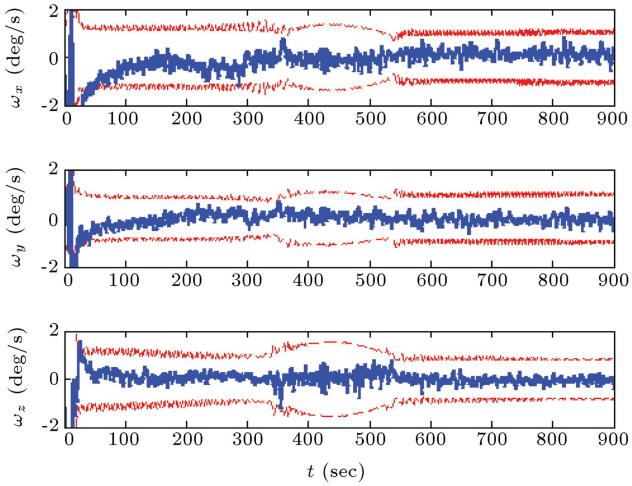

Figure 5. Body angular velocity estimation errors in MMUKF with $\pm$ 3σ error bounds.

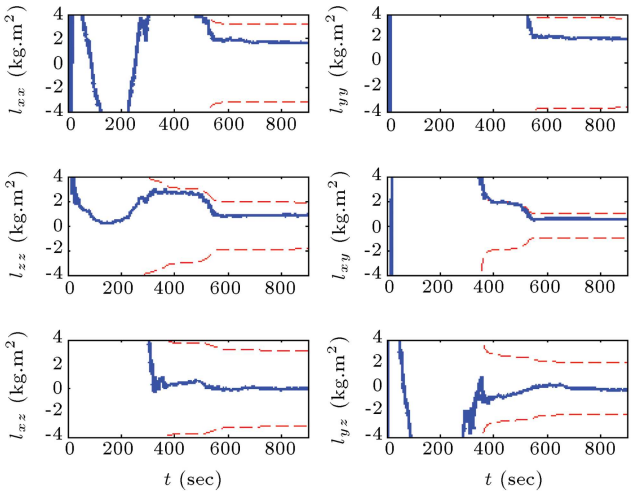

Figure 6. Moments of inertia estimation errors in MMUKF with $\pm$ 3σ error bounds.

ciency. Despite similar accuracy level of the three algorithms, mean average run time of the MMUKF over 10 simulations was only about 1615 sec, as opposed to 3588 sec for the MUKF, and 4957 sec for standard UKF. This indicates that the MMUKF has made a 68% reduction in the run time relative to standard UKF, and 55% relative to MUKF which is definitely more efficient and advantageous for online applications. This problem is solved on a PC computer with 4 G RAM and a CPU of 2.53 GHz.

To demonstrate the efficiency of the proposed MMUKF, the results of its Monte Carlo simulations are presented. Figures 4 through 9 show estimation errors of state vector (solid lines) along with $\pm 3\sigma$ error bounds (dashed lines) taken from the covariance matrix at every time step. This convergence verifies good performance of the utilized algorithm and shows that each variable has a different convergence time constant. Figures 4 and 5 show that attitude and body angular velocity estimation errors converge to within their respective 3σ value after only 40 sec that indicates MMUKF is performing in a near optimal fashion. Similarly, Figures 6 through 8 show convergence to 3σ bounds in 60 sec for MOI estimation, 30 sec for scale factors and 20 sec for misalignment parameters. In contrast to fast convergence of the states and mentioned system parameters, it takes about 300 sec to have a converged bias estimation error. Table 4 also summarizes the root mean square error of state vector. It is notable that to calculate the attitude estimation error, error quaternion is calculated first as $\{\delta \mathbf{q}\} = \mathbf{q} \otimes \hat{\mathbf{q}}^{-1}$. Since the fourth elements of quaternion is the scalar part; according to quaternion definition that $q_4 = \cos(\phi/2)$, and ϕ is the rotation angle, error estimation of rotation angle is $\delta\phi = 2\cos^{-1}(\{\delta \mathbf{q}\}_4)$.

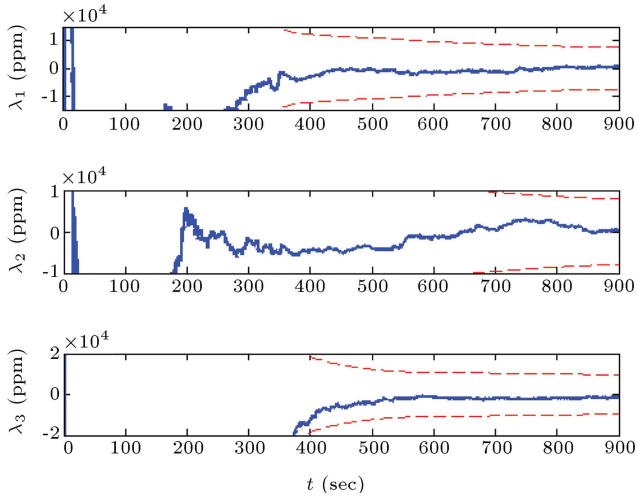

Figure 7. Scale factors estimation errors in MMUKF with $\pm$ 3σ error bounds.

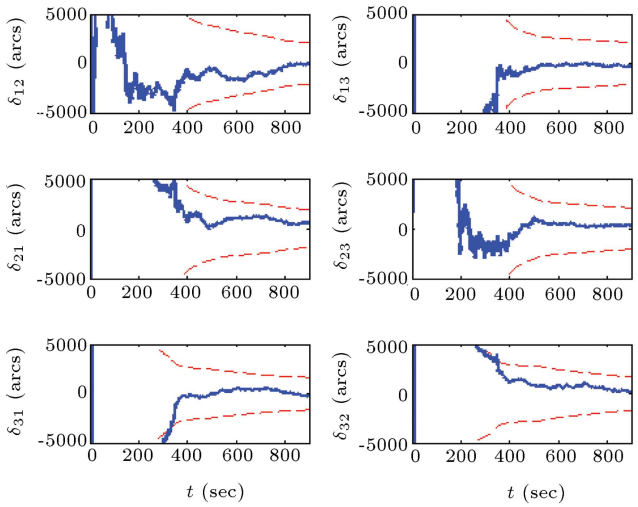

Figure 8. Misalignments estimation errors in MMUKF with $\pm$ 3σ error bounds.

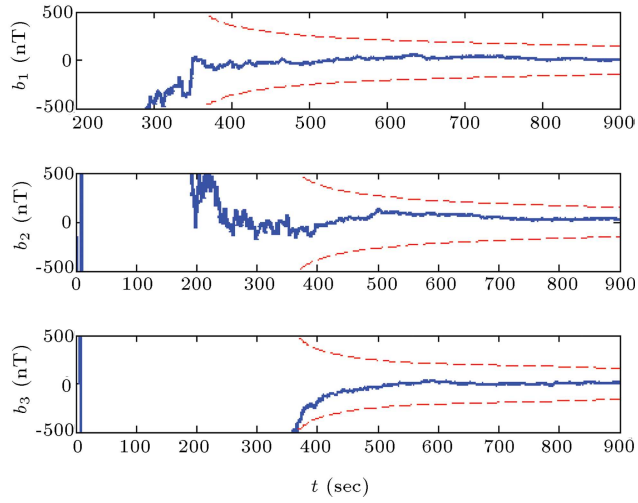

Figure 9. TAM bias estimation errors in MMUKF with $\pm$ 3σ error bounds.

6. Conclusion

This paper has focused on concurrent Attitude Determination (AD), Parameter Identification of dynamic system (PI) and Measurement Sensor Calibration (MSC). Accordingly, moments of inertia tensor for the attitude dynamic system, scale factor, misalignment and biases of the Three-Axis-Magnetometer (TAM) is recursively estimated based on central data fusion of TAM and the sun sensor. As the governing model of the considered problem is a mixture of linear and nonlinear equations, or in other words a partially linear problem, an advanced marginal unscented Kalman filter consisting of Kalman Filter (KF) and a Modified Unscented Kalman Filter (MUKF) is proposed and introduced as Marginal Modified UKF (MMUKF). MMUKF is implemented as a robust tool to reach acceptable accurate estimations. MMUKF utilizes only 14 sigma points to estimate a full 25-dimensional state vector, while standard UKF needs 52 sigma points and MUKF requires 26 sigma points for the same problem. Application of MMUKF reduces the run time to about 68% with respect to the standard UKF, while preserving the same accuracy level.

Stability and success of the proposed system and filter algorithm are demonstrated via a Monte Carlo analysis for a LEO satellite. The achieved levels of accuracy, through the proposed scheme, satisfy the qualification requirement of navigation, and control subsystems of LEO satellites.

Nomenclature

$\vec{b}$	Bias vector (nT)
C_D	Drag coefficient
I_B^B	Moment of inertia tensor in body axes (kg.m^2)
$\{\mathbf{q}\}$	Quaternion parameters
r	Orbital radius of the satellite (m)
S	Cross section area (m^2)
$\vec{\omega}_{\mathrm{BI}}$	Angular velocity of body frame relative to inertial frame (rad/s)
$\vec{\tau}$	Total exerted torques (N.m)
$\vec{\tau}_c$	Control torque (N.m)
$\vec{\tau}_d$	Disturbance torque (N.m)
ρ	Air density (kg/m^3)
v	Magnitude of the satellite velocity (m/s)
λ	Scale factor
δ	mmisalignment parameter

$[.]^B$ Quantity expressed in body coordinate system

References

1. Wertz, J.A. and Lee, A.Y. "In-flight estimation of the cassini spacecraft's inertia tensor", *Journal of Spacecraft and Rockets*, **39**(1), pp. 153-155 (2000).
2. Zarringhalam, R., Rezaeian, A., Melek, W., Khajepour, A., Chen, S.-K. and Moshchuk, N. "A comparative study on identification of vehicle inertial parameters", *American Control Conference*, Montreal, Canada (2012).
3. Jun, B-E., Bernstein, D.S. and McClamroch, N.H. "Identification of the inertia matrix of a rotating body based on errors-in-variables models", *International Journal of Adaptive Control and Signal Processing* (2009).
4. Norman, M.C., Peck, M.A. and O'shaughnessy, D.J. "In-orbit estimation of inertia and momentum-actuator alignment parameters", AAS 11-164 (2010).
5. Mohammed, A.M. Si, Boudjemai, A., Bentoutou, Y., Bellar, A., Roubache, R. and Taleb, N. "Kalman filtering for microsatellite attitude determination in orbit results", *6th International Conference on Recent Advances in Space Technologies (RAST)*, Istanbul, Turkey, pp. 383-387 (2013).
6. Pittelkau, M.E. "Kalman filtering for spacecraft system alignment calibration", *Journal of Guidance, Control and Dynamics*, **24**(6), pp. 1187-1195 (2001).
7. Ma, G-F. and Jiang, X-Y. "Unscented Kalman filter for spacecraft attitude estimation and calibration using magnetometer measurements", *Proceedings of the Fourth International Conference on Machine Learning and Cybernetics* (2005).
8. Wang, P. Zhang, Y-C. and Qiang, W-Y. "Research on the algorithm of on-orbit calibration based on gyro/star-sensor", *Proceedings of the Fifth International Conference on Machine Learning and Cybernetics* (2006).
9. Kim, E. and Bang, H-C. "Bias estimation of magnetometer using genetic algorithm", *International Conference on Control, Automation and Systems* (2007).
10. Lai, K-L., Crassidiss, J.L. and Harman, R.R. "In-space spacecraft alignment calibration using the unscented filter", *AIAA Guidance, Navigation and Control Conference*, Austin (2003).
11. Kim, Y.V., Di Filippo, K.J. and Ng, A. "On the calibration of satellite on-board magnetometer", *The Fourth International Conference on Control and Automation (ICCA'03)* (2003).
12. Crassidiss, J.L., Lai, K.-L. and Harman, R.R. "Real-time attitude-independent three-axis magnetometer calibration", *AIAA Journal of Guidance, Control and Dynamics*, **28**(1), pp. 115-120 (2005).
13. Soken, H.E. and Hajiyev, C. "Reconfigurable UKF for in-flight magnetometer calibration and attitude parameter estimation", *18th IFAC World Congress*, (2011).
14. Kutlu, A., Hacryev, C. and Tekinalp, O. "Attitude determination and rotational motion parameters identification of a LEO satellite through magnetometer and sun sensor data", *International Conference on Recent Advances in Space Technologies* (2007).
15. Myung, H., Yong, K-L. and Bang, H. "Hybrid estimation of spacecraft attitude dynamics and rate sensor alignment parameters", *International Conference on Control, Automation and Systems* (2007).
16. Sidi, M.J., *Spacecraft Dynamics and Control*, Cambridge University Press (1997).
17. Shuster, M.D. "A Survey of attitude representations", *Journal of the Astronautical Sciences*, **41**(3) (1993).
18. Zipfel, P.H. "Modeling and simulation of aerospace vehicle dynamics", *AIAA Education Series* (2000).
19. Fan, C. and You, Zh., "Highly efficient sigma point filter for spacecraft attitude and rate estimation", *Mathematical Problems in Engineering* (2009) doi: 10.1155/2009/507370.
20. Briers, M., Maskell, S.R. and Wright, R. "A rao-blackwellised unscented Kalman filter", *in Proc. 6th International Conference of Information Fusion*, Queensland, Australia (2003).
21. Julier, S.J. and Uhlmann, J.K. "A new extension of the Kalman filter to nonlinear systems", in *Proc. of AeroSense: The 11th Int. Symposium on Aerospace/Defense Sensing, Simulation and Controls*, (1997).
22. Li, W.-Ch., Wei, P. and Xiao, X.-C. "Novel simplex unscented transform and filter", *Journal of Electronic and Technology of China*, **6**(1) (2008).
23. Finlay, C.C., Maus, S., Began, C.D. et al. "International geomagnetic reference field: the eleven generation", *Geophys. J. Int.*, **183** (2010).

Biographies

Maryam Kiani holds a BS degree in aerospace engineering from Amirkabir University of Technology (2006), and an MS degree in flight dynamics and control from Sharif University of Technology (2008). Currently, she is a PhD student at Sharif University of Technology. Her research interests are focused on

nonlinear filtering techniques and system identification for satellite and space systems.

Seid H. Pourtakdoust received his PhD in aerospace engineering from the University of Kansas, USA, in 1989. He is currently a full professor at Sharif University of Technology, Tehran, Iran. His main areas of research and expertise are focused on applied optimal control with emphasis on space missions and optimization. He is also interested in aeroelastic modeling and simulation of aerospace vehicles and has published many scientific papers.